Journal of Colloid and Interface Science 357 (2011) 345–353

Contents lists available at ScienceDirect

Journal of Colloid and Interface Science

www.elsevier.com/locate/jcis

Non-ionic, thermo-responsive DEA/DMA nanogels: Synthesis, characterization, and use for DNA separations by microchip electrophoresis

Xihua Lu [a], Mingyun Sun [a,b], Annelise E. Barron [a,b,*]

[a] Department of Chemical and Biological Engineering, Northwestern University, Evanston, IL 60208, United States
[b] Department of Bioengineering, Stanford University, 318 Campus Drive, Clark Center Room S170, Stanford, CA 94305-5444, United States

ARTICLE INFO

Article history:
Received 30 October 2010
Accepted 22 January 2011
Available online 1 February 2011

Keywords:
Nanogels
DEA
DMA
LCST
Microchip electrophoresis
DNA separations

ABSTRACT

Thermo-responsive polymer "nanogels" (crosslinked hydrogel particles with sub-100 nm diameters) are intriguing for many potential applications in biotechnology and medicine. There have been relatively few reports of electrostatically neutral, thermosensitive nanogels comprising a high fraction of hydrophilic co-monomer. Here we demonstrate the syntheses and characterization of novel, non-ionic nanogels based on random *N*,*N*-diethylacrylamide (DEA)/*N*,*N*-dimethylacrylamide (DMA) copolymers, made by free-radical, surfactant-free dispersion polymerization. The volume-phase transition temperatures of these DEA/DMA nanogels are strongly affected by co-monomer composition, providing a way to "tune" the phase transition temperature of these non-ionic nanogels. While DEA nanogels (comprising no DMA) can be obtained at 70 °C by standard emulsion precipitation, DEA/DMA random co-polymer nanogels can be obtained only in a particular range of temperatures, above the initial phase transition temperature and below the critical precipitation temperature of the DEA/DMA copolymer, controlled by co-monomer composition. Increasing percentages of DMA in the nanogels raises the phase transition temperature, and attenuates and broadens it as well. We find that concentrated DEA/DMA nanogel dispersions are optically clear at room temperature. This good optical clarity was exploited for their use in a novel DNA sieving matrix for microfluidic chip electrophoresis. An ultrafast, high-efficiency dsDNA separation was achieved in less than 120 s for dsDNA ranging from 75 bp to 15,000 bp.

1. Introduction

Nanogels, *i.e.*, hydrogel nanoparticles with diameters in the range of tens to hundreds of nanometers, are attracting interest and investigations [1–4]. With their extremely small size and high surface area-to-volume ratios, thermo-responsive nanogels can exhibit unusually rapid responses to micro-environmental stimuli such as temperature [2] or pH, relative to bulk gels made from the same materials [5]. Hydrogel nanoparticles have been tested for controlled drug release [6,7], as the basis for novel DNA sieving networks for microchannel electrophoresis [8], and for environmental control [9] or optical uses [10,11]. A variety of thermo-responsive nanogels are reported that exhibit reversible volume-phase transitions [4,12]. Typically, below the nanogels' volume-phase transition temperature (VPTT) the polymer chains that form the gel particles are hydrogen-bonded with water molecules so that the nanogel material is well hydrated and swollen in an aqueous milieu. Above the VPTT, the polymers undergo thermodynamically driven coil-to-globule transitions. This initially nanoscale phase separation can occur almost as quickly as the coil-to-globule transition of individual polymer chains, yielding fast nanogel volume transitions at or above the VPTT.

Among various thermo-responsive poly(*N*-alkyl-substituted acrylamide) nanogels that have been studied [4,13,14], poly(*N*-isopropylacrylamide) (polyNIPA) nanogels have been the most extensively investigated [15–17]. NIPA-based nanogels are typically synthesized by emulsion precipitation polymerization at 70 °C [2]. Similar to linear NIPA polymers, polyNIPA nanogels exhibit a reversible volume-phase transition at a VPTT of ~32 °C. Above the VPTT, they typically remain stably dispersed in the aqueous solution, in most cases due to electrostatic repulsion between sulfate moieties incorporated into the nanogels when polymerization

Abbreviations: DEA, *N*,*N*-diethylacrylamide; DMA, *N*,*N*-dimethylacrylamide; MALLS, multi-angle static laser light scattering; NIPA, *N*-isopropylacrylamide; PCS, photon correlation spectroscopy; DLS, dynamic light scattering; VPTT, volume-phase transition temperature; LCST, lower critical solution temperature; PDI, polydispersity index.

* Corresponding author at: Department of Bioengineering, Stanford University, 318 Campus Drive, Clark Center Room S170, Stanford, CA 94305-5444, United States. Fax: +1 650 723 9801.

E-mail addresses: xhlu2002@gmail.com (X. Lu), mingyuns@gmail.com (M. Sun), aebarron@stanford.edu (A.E. Barron).

0021-9797/$ - see front matter © 2011 Elsevier Inc. All rights reserved.
doi:10.1016/j.jcis.2011.01.079

was initiated by ammonium persulfate (APS) [4]. The VPTT of NIPA-based nanogels can be varied by the incorporation of a small amount of an ionic co-monomer such as acrylic acid (AA) or methacrylic acid (MAA) [5,18]. These charged co-polymer nanogels exhibit both temperature- and pH-induced volume-phase transitions.

In addition to polyNIPA, poly(*N*,*N*-diethylacrylamide) (polyDEA) is another thermo-responsive polymer that shows an LCST near 30 °C [19,20]. Wu et al. investigated the effects of co-monomer composition on the formation of the meso-globular phase of DEA co-polymers using laser light scattering [21]. Zhu and coworkers studied the enhanced thermosensitivity of *N*,*N*-diethylacrylamide/2-hydroxyethyl methacrylate (DEA/HEMA) nanogels [22]. Barron et al. showed that the incorporation of the neutral hydrophilic co-monomer DMA into random DMA/DEA co-polymers, in increasing amounts, leads to a controlled shift of the VPTT to higher temperatures [23]. The ability to control the VPTT of these non-ionic, thermo-responsive copolymers can have important consequences for their application [24]. For example, by exploiting the dramatic viscosity drop associated with the volume-phase transitions of linear DEA/DMA co-polymer solutions, Barron and coworkers [23] created a novel class of microchannel DNA sequencing matrices with a thermally controlled viscosity switch, capable of decoupling high-pressure microchannel loading and electrophoretic DNA sequencing separation performance for these otherwise highly viscous solutions (7% w/v) of entangled, linear, high-molar mass DEA/DMA co-polymers ($M_w \sim 4$ M g/mol) [23].

Non-ionic, thermosensitive nanogels with a high molar composition of highly hydrophilic co-monomers were reported for the first time only recently. Zhou and coworkers synthesized poly(ethylene glycol) (PEG)-based, thermosensitive core–shell nanogels, and studied their use for cancer cell imaging and treatment [25,26]. Their PEG-based nanogel shell was composed of 2-(2-methoxyethyoxy)ethyl methacrylate (MEO_2MA) and oligo(ethylene glycol)methyl ether methacrylate (MEO_5MA, M_n = 300 g/mol) in 1:2 molar ratio. Although the nanogel shell had a high composition of the more hydrophilic MEO_5MA, poly(MEO_5MA) itself has a sufficient level of hydrophobicity to also form thermosensitive homo-polymer with an LCST of about 60 °C [27,28]. Gu's group synthesized non-ionic, thermosensitive NIPA/AAm (acrylamide) nanogels with a maximum hydrophilic AAm composition of less than 20 wt.% (AAm/NIPA = 0.2 g/1 g) [29]. The AAm content of these NIPA/AAm nanogels was higher than the earlier published result of Pelton and Chibante in 1986 [30].

In this study, we show for the first time, that the VPTT of DEA-based nanogels can be tuned through the copolymerization of DEA with a high composition of a hydrophilic, non-ionic DMA co-monomer. DMA is sufficiently hydrophilic that its homo-polymers do not demonstrate any LCST transitions in water below 100 °C. The chemical structure of DMA is similar to that of DEA, as shown in Fig. 1. Aqueous solutions of linear poly(*N*,*N*-dimethylacrylamide) (polyDMA) are soluble in water up to 100 °C, while aqueous solutions of linear poly(*N*,*N*-diethylacrylamide) (polyDEA) exhibit an LCST at around 30 °C. Random DMA/DEA copolymers exhibit intermediate phase transitions [23]. DMA-based homo-polymers and co-polymers find many practical uses, such as in contact lenses, and as sieving networks for microchannel DNA sequencing. One reason for this relates to stability: in mildly alkaline or acidic conditions, DMA is much more resistant to hydrolysis than acrylamide [31]. High-molar mass DMA homo-polymers and DEA/DMA co-polymers have been used in electrophoresis media for DNA sequencing by capillary electrophoresis [23]. For this application, PDMA offers two significant advantages over linear polyacrylamide: (1) at necessary polymer concentrations (2–6% w/v), its entangled polymer solutions have relatively lower viscosity, and (2) polyDMA spontaneously adsorbs to glass, via physical and entropic driving forces, to form a capillary coating that suppresses electroosmotic flow and enhances DNA separation performance [32].

We synthesized polyDEA nanogels at 70 °C *via* emulsion precipitation polymerization, following an approach typically used to create polyNIPA nanogels, which have a VPTT very close to that of polyDEA. However, when we attempted to synthesize DMA/DEA nanogels by a similar method, we found that mixed DEA/DMA monomer solutions tend to form a macroscopic precipitate shortly after the initiation of polymerization at 70 °C, and this occurred over a wide range of DEA/DMA feed ratios, ranging from 70%/30% (w/w) to 40%/60% (w/w). We therefore explored alternative synthesis conditions. We discovered that the synthesis of DEA/DMA nanogels must be carried out within a narrow range of reaction temperatures that depends on copolymer composition, and which is above the initial volume-phase transition temperature and below the critical precipitation temperature at which DEA/DMA copolymer particles form a macroscopic precipitate. We varied the reaction temperature, crosslinker concentration, monomer ratio, and reaction time to investigate the effect of synthesis conditions on the size and size distribution of the nanogels. The weight-average molecular weight (M_w) and gyration of radius (R_g) were measured by multi-angle static light scattering. The temperature-dependent phase transition behaviors of the resulting DEA/DMA nanogels, both in water and in aqueous NaCl solutions, were studied by dynamic light scattering and visible-light spectrophotometry.

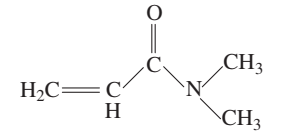

N,*N*-dimethylacrylamide (DMA)

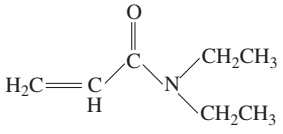

N,*N*-diethylacrylamide (DEA)

Fig. 1. Chemical structures of *N*,*N*-diethylacrylamide (DEA) and *N*,*N*-dimethylacrylamide (DMA).

2. Materials and methods

2.1. Materials

Ultrapure (>99.5%) monomers of *N*,*N*-diethylacrylamide (DEA) and *N*,*N*-dimethylacrylamide (DMA) were purchased from Monomer–Polymer and Dajac Labs (Feasterville, PA) by custom order. The crosslinker methylene-bis-acrylamide (Bis), ammonium persulfate (APS), sodium dodecyl sulfate (SDS) and *N*,*N*,*N*′,*N*′-tetramethylethylenediamine (TEMED) were all purchased from Amresco (Solon, OH) in High purity. Triply distilled, deionized water was used throughout.

*Φ*X 174 RF DNA/Hae III Fragments and 1 Kb DNA Extension Ladder were obtained from Invitrogen (San Diego, CA). The buffer used in all experiments was 0.5 × TTE (50 mM tris(hydroxymethyl)aminomethane (Tris), 50 mM *N*-tris(hydroxymethyl)methyl-3-aminopropanesulfonic acid (TAPS), 2 mM ethylenediaminetetraacetic acid (EDTA).) Tris was obtained from ISC BioExpress Inc. (Kaysville,

UT), TAPS from Fisher Scientific (Pittsburgh, PA), and EDTA from Sigma (St. Louis, MO). Polymer matrices included some fraction of dissolved hydroxyethyl cellulose (HEC) from Polysciences, Inc. (Warrington, PA), as well as linear polyacrylamide (LPA) and the DEA/DMA nanogels (42% DEA/58% DMA, w/w) synthesized in our laboratory. The polymers that were used as a dynamic (physically adsorbed) microchannel wall coating (poly(*N*-hydroxyethylacrylamide) (polyHEA)) were synthesized in our laboratory as well and were used to suppress electroosmostic flow (EOF) in microfluidic electrophoresis. Ethidium bromide (EtBr) dye was obtained from Fisher Scientific (Pittsburgh, PA).

2.2. Synthesis of the nanogels

PolyDEA nanogels were synthesized *via* emulsion precipitation polymerization. In a typical synthesis, 2.4 g DEA monomer, 0.08 g SDS surfactant and 0.24 g Bis were dissolved in 187.6 g water. The solution was stirred under nitrogen. After the solution was brought to 70 °C under nitrogen, 10 ml of a 0.01 g/ml aqueous APS solution were added to initiate polymerization. The polymerization was carried out at 70 °C for 4 h under nitrogen. The resultant PDEA nanogels were dialyzed through cellulose acetate membranes (Carolina Biological Supply Company, NC) for 10 days to remove unreacted monomer, small molecules and SDS surfactant.

The DEA/DMA nanogels were synthesized *via* surfactant-free emulsion precipitation polymerization. DEA/DMA nanogels were prepared from 2.86 g of DEA and DMA monomer with four different DEA/DMA compositions (70%/30%, 60%/40%, 50%/50%, 40%/60%, w/w), 0.286 g Bis (10 wt.% of total feed amount of DEA and DMA), and 0.1 g APS. The DEA and DMA monomers and BIS crosslinker were dissolved in 187.7 g water. Following the addition of APS, the copolymerization was carried out, at different reaction temperatures based on the various monomer compositions. Copolymer nanogels were dialyzed (Carolina Biological Supply Company, NC) for 10 days to remove unreacted monomers and small molecules. The dialyzed nanogels were freeze-dried for later re-dispersion and study. The specific synthesis conditions used are given in Table 1.

2.3. NMR measurements

^{1}H NMR spectroscopy with a Varian Inova 500 (Walnut Creek, CA) was utilized to determine the actual molar ratio of each monomer incorporated into the DEA/DMA nanogels. In the individual DEA and DMA monomers, there are two CH_3 groups. However, in the two monomers these CH_3 groups reside in unique chemical environments. The DEA/DMA ratio of the nanogels thus can be measured *via* the integration of the NMR signals corresponding to the ^{1}H of the CH_3 groups in DEA and DMA, respectively. The freeze-dried DEA/DMA nanogels (0.04 g) were dissolved in 1 ml of D_2O solvent. ^{1}H NMR (500 MHz, D_2O) was then performed, measuring δ (ppm): 1.10 ($2CH_3$ of DEA, br s), 2.94 ($2CH_3$ of DMA, br s). DEA/DMA nanogels with four different compositions were studied, as shown in Table 1.

2.4. Multi-angle laser light scattering (MALLS) and dynamic light scattering (DLS)

In order to minimize the effect of dust, a 0.02 μm filter (Whatman) was used to remove possible dust in DI water and 0.8 μm filter (Whatman) removed any dust in the nanogel dispersion preparations. The physical properties of resultant DEA/DMA nanogels were characterized by MALLS and DLS [33–35] and are given in Table 2. All $\langle R_g \rangle$ and M_w values were calculated from Zimm plots for the nanogel samples determined from MALLS data. By use of the Berry formalism for data analysis [32], and a first-order angle fit and a second-order concentration fit, the calculated values showed an error of no more than 5%. All $\langle R_h \rangle$ values were determined from five independent DLS measurements using a detector angle of 23° at 20 °C. The $\langle R_h \rangle$ error was also less than 5%. The instruments and measurement conditions in detail are described in the Supporting information.

2.5. Microchip electrophoresis

Microfluidic chip electrophoresis was conducted using a custom-built system in our laboratory which has a highly sensitive multi-color laser-induced fluorescence (LIF) detector, capable of detecting ~3 pM fluorescein [36]. Glass microchips (T8050) were obtained from Micronit (Enschede, The Netherlands) and had a standard, 100 μm "offset T" injector, an 8-cm separation distance, and 50-μm wide, 20-μm deep channels. Microchannels were internally coated, *via* simple physical polymer adsorption, using a 0.1% (w/w) poly-*N*-hydroxyethylacrylamide (pHEA) aqueous solution, after a 15-min surface pretreatment with 1 M HCl in water. DNA samples were diluted to 5 μg/ml with deionized water. Appropriate amounts of matrix polymer materials were added into 0.5 × TTE buffer for the obtainment of good separation performance for both small and large DNA fragments. DNA samples and polymer matrix solutions were spiked with 1 μM EtBr. DNA samples were electrokinetically injected with an applied voltage 200 V for 20 s. The separation electric field strength was 300 V/cm.

3. Results and discussion

3.1. Synthesis of polyDEA and DEA/DMA nanogels

Thermo-responsive nanogels are usually synthesized at a temperature well above the lower critical solution temperature (LCST) of the corresponding linear polymers. This is because at elevated temperatures, thermosensitive polymer chains typically can form stably dispersed nanospheres above the LCST in aqueous media, with or without the need for added surfactant, depending on the material and solvent conditions. The two most common nanogel synthesis methods include direct crosslinking of the collapsed polymer chains [3] and free-radical polymerization of monomers in the presence of a crosslinker [4]. The latter method is usually referred to as emulsion precipitation polymerization. Many classes of nanogels have been synthesized *via* emulsion precipitation

Table 1
Synthesis conditions of polyDEA nanogels and DEA/DMA nanogels.

Samples	DEA/DMA feed ratio		DEA/DMA feed ratio from ^{1}H NMR		Reaction T (°C)	TEMED (g)	SDS (g)
	(wt.%/wt.%)	(mol%/mol%)	(wt.%/wt.%)	(mol%/mol%)			
PolyDEA	100/0	100/0	100/0	100/0	70	0	0.08
DEADMA73	70/30	64.5/35.5	71.4/28.6	65.8/34.2	37	0.05	0
DEADMA64	60/40	53.9/46.1	60.9/39.1	54.7/45.3	46	0.05	0
DEADMA55	50/50	43.8/56.2	52.1/47.9	45.6/54.4	54	0	0
DEADMA46	40/60	34.1/65.9	40.9/59.1	34.9/65.1	65	0	0

Table 2
Laser light scattering characterization of polyDEA nanogels and DEA/DMA nanogels.

Samples	LCST (°C)	$\langle R_h \rangle$[a] (nm)	$\langle R_g \rangle$ (nm)	$\langle R_g/R_h \rangle$	PDI[b]	dn/dc	M_w ($\times 10^7$) (g/mol)
PolyDEA	26	194	165	0.85	0.16	0.185	19.2
DEADMA73	45	226	275	1.22	0.40	0.165	3.24
DEADMA64	52	208	261	1.25	0.41	0.164	2.65
DEADMA55	58	243	288	1.19	0.44	0.167	3.89
DEADMA46	67	199	243	1.22	0.46	0.162	2.21

Note.
[a] Average hydrodynamic radii were measured at small measurement angle 23°.
[b] PDI denotes polydispersity or relative standard deviation of resulting nanogels: the ratio of the standard deviation in R_h to the average hydrodynamic radius.

polymerization, including core–shell NIPA nanogels [2], pH-sensitive NIPA/MAA co-polymer nanogels [5], and polyampholyte nanogels [13].

In order to create non-ionic DEA/DMA nanogels with tunable VPTTs, we first attempted to develop a synthesis protocol based on emulsion precipitation polymerization at 70 °C. Using this approach, homogeneous polyDEA nanogels were indeed obtained (see below). However, when we attempted to use this method to create co-polymer nanogels, we found that in aqueous SDS solution, the DEA/DMA copolymers rapidly aggregated to form a macroscopic precipitate, shortly after the initiation of polymerization at 70 °C. This occurred over a wide range of DEA/DMA compositions, from 70 wt.% to 40 wt.% of DEA. If surfactant was used for emulsion precipitation polymerization of DMA/DEA copolymers at lower temperatures, nanogels were formed but were quite polydisperse (results not shown). We preferred not to use surfactant if it was not necessary, to eliminate a requirement for its later removal. Subsequent experimental studies showed that the synthesis of stable DEA/DMA nanogels could be achieved only in a narrow range of reaction temperatures, above the respective initial phase transition temperature and below the individual critical precipitation temperature above which DEA/DMA copolymer chains form a macroscopic precipitate. In contrast to the previous DEA nanogel synthesis at a temperature well above the LCST, this controlled synthesis temperature of DEA/DMA nanogels is just a few degrees above the initial volume-phase transition temperature, which is a novel finding.

Pelton et al. have reported that the optimal synthesis temperature of preparing poly(*N*-isopropylacrylamide) nanogels is above 50 °C, which is significantly higher than a LCST of 32 °C [37,38]. Similar to the LCST of linear DEA/DMA copolymers, the critical precipitation temperature of DEA/DMA nanogels depends on the copolymer composition: the higher the DMA content, the higher the critical precipitation temperature. Thus, DEA/DMA nanogels with different compositions cannot be created at the same reaction temperature; the reaction temperature must be varied with the comonomer composition. This is likely due to the differing balance of hydrophobic and physical association tendencies of the DEA/DMA copolymer chains, as affected by composition, above the critical precipitation temperature. Nanogels with a significant fraction of DMA, once formed, apparently have a stronger affinity for other nanogels, so that they form a macroscopic precipitate at 70 °C. Barker et al. [39] investigated the effects of the hydrophilic co-monomer DMA on the segmental mobility of linear NIPA/DMA copolymers *via* time-resolved anisotropy measurements (TRAMS). They reported that the incorporation of the more hydrophilic DMA reduces the extent of the collapse transitions of linear NIPA/DMA copolymers above the LCST, and that an increase in DMA content greatly enhances the segmental mobility of NIPA/DMA copolymers above the initial volume-phase transition temperature. In contrast to NIPA/DMA copolymers, homogeneous polyNIPA was found to exhibit a sharp decrease in segmental mobility upon its strong collapse above the LCST.

In the present study, DEA/DMA copolymer chains would be expected to behave somewhat similarly to NIPA/DMA copolymer chains. We were aware that at higher reaction temperatures, the fast mobility and strong hydrophobic association of the copolymer segments of the resulting DEA/DMA particles above the phase transition temperature could lead to the rapid formation of a macroscopic precipitate. For this reason, the synthesis temperatures of DEA/DMA nanogels with different compositions had to be varied to modulate the strength of the hydrophobic effect (see Table 1). When synthesis conditions had been optimized for each unique DEA/DMA composition and surfactant was omitted from the reaction, discrete nanogels could be obtained, as signaled by the appearance of a bluish tint to the clear solutions. No precipitation occurred under the optimal synthesis conditions shown in Table 1.

3.2. Physical characterization of the nanogels

Static light-scattering studies of the synthesis products show that polyDEA nanogels have by far the highest average molar mass (1.92×10^8 g/mol), due to the more highly packed polymer chains that form during synthesis, with a ratio of $R_g/R_h \sim 0.84$ [40]. The weight-average molar masses of the DEA/DMA co-polymer nanogels, on the other hand, ranged from 2.21×10^7 to 3.89×10^7 g/mol. The corresponding R_g ranges from 243 to 288 nm and R_h from 199 to 243 nm. The ratios of R_g/R_h of DEA/DMA nanogels are around 1.2, indicating that resulting DEA/DMA nanogels have much less tightly packed polymer chains than polyDEA nanogels [40,41]. Compared to the relatively low R_g/R_h of polyDEA nanogels, the higher R_g/R_h ratios of DEA/DMA nanogels may be attributed to two synthesis factors: the use of a lower polymerization temperature, not very far above the respective copolymer LCSTs; and the high mobility of the DMA portions of the more hydrophilic DEA/DMA polymer chains. These factors will lead to the creation of loosely packed DEA/DMA polymer chains in individual nanogels and hence, broader polydispersity, as observed by DLS, as shown in Table 2. The polyDEA nanogels have the narrowest size distribution, which can be attributed to fast particle nucleation at the relatively high reaction temperature of 70 °C. The polydispersities of the DEA/DMA nanogels ranged from 0.40 to 0.46. Lyon et al. reported a similarly broad polydispersity (0.42) for their poly(ethylene glycol) (PEG)-modified NIPA nanogels, which they attributed to the incorporation of the hydrophilic PEG-monomethacrylate [42]. An interesting consequence of the DEA/DMA nanogel made by this method is their optical transparency, which can have advantages in some optical applications.

In order to investigate the effects of various synthesis parameters on the size and size distribution of the DEA/DMA nanogels, we characterized nanogels that were synthesized over a range of reaction temperatures, reaction times, and with different crosslinker concentrations. DEA/DMA co-polymer nanogels with a composition of 60% DEA/40% DMA (w/w) were synthesized at 42 °C, 44 °C, and 46 °C. In contrast to a slight decrease of nanogel size with increasing reaction temperature seen in NIPA nanogel

synthesis [43], the average hydrodynamic diameter of DEA/DMA nanogels increases with increasing reaction temperature, as shown in Fig. 2. Our experiments show that DEA/DMA (70%/30%) nanogels polymerized at 37 °C for 2 or 4 h in the presence of catalyst TEMED exhibit little difference in their sizes and size distributions (data not shown). A similar effect of reaction time on the size of polyNIPA microgels has been previously reported [4,44], Pelton [4] found that the sizes of microgels they synthesized remained almost invariant after one hour of polymerization, even at a lower reaction temperature of 50 °C.

The crosslinking density is another important synthesis parameter that usually alters the swelling ratio of synthetic nanogels. For instance, Duracher et al. studied the influence of crosslinking density on the sizes of polyNIPA nanogels [44], and reported that an increase in crosslinking density had little effect on nanogel size below the VPTT, while the size of the collapsed nanogels increased with an increase of crosslinker density above the VPTT. We synthesized DEA/DMA nanogels with 70 wt.% DEA and 30 wt.% DMA at 37 °C, using crosslinker concentrations of 2.5 wt.%, 5.0 wt.%, and 10 wt.% of the total amount of DEA and DMA monomers. The size distributions we obtained for nanogels with different extents of crosslinking are shown in Fig. 3. Our results show that the size of the DEA/DMA nanogels determined at 20 °C increases with increasing crosslinker concentration, but there is little effect of the crosslinking density on the size distribution, which remains relatively broad. The variation of nanogel size with crosslinker density may be related to the reaction temperature at which the nanogels are created. In the synthesis of DEA/DMA nanogels, the ideal reaction temperature is just a few degrees above the initial volume-phase transition temperature. The growth of the polymer chains in each nanogel is dependent on the crosslinker concentration, such that higher crosslinker concentration in solution can capture and hold more polymer chains, to form larger nanogels.

3.3. Characterization of the VPTTs of DEA/DMA co-polymer nanogels

The VPTTs of co-polymer nanogels previously reported by others have been varied *via* the incorporation of ionic co-monomers [5,18]. The introduction of ionic groups into nanogels presents two limitations. First, only a small amount of ionic co-monomer can be introduced, since the incorporation of larger amounts leads to a loss of the thermosensitive phase behavior of the nanogels. For example, for a composition of more than 10 mol% acrylic acid (AA), the VPTT of NIPA/AA nanogels disappears at pH 7.4, because the AA components include ionic groups that strongly absorb and interact with water [18,45]. Secondly, it is expected that nanogels with ionic groups are not suitable for some applications of interest, such as electrophoretic

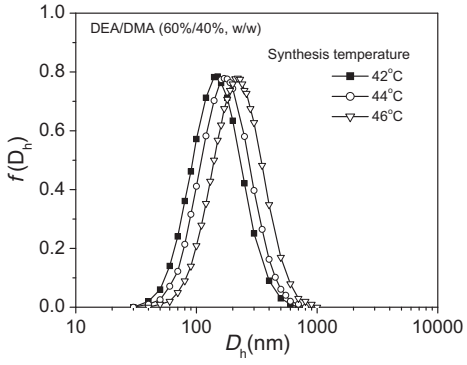

Fig. 2. The size distribution of the DEA/DMA (60%/40%, w/w) nanogels at 20 °C, synthesized at the reaction temperatures of 42 °C, 44 °C, 46 °C.

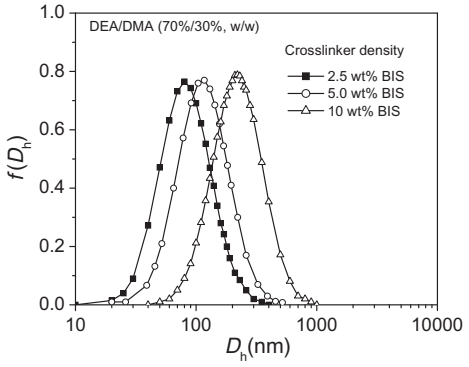

Fig. 3. The size distribution of DEA/DMA (70%/30%, w/w) nanogels at 20 °C with crosslinker concentrations of 2.5 wt.%, 5.0 wt.%, and 10.0 wt.% of feed monomer DEA, and DMA.

DNA separations, which require an electrostatically neutral polymer matrix [46,47]. Only a very few studies have focused on the tunable VPTT of non-ionic co-polymer nanogels [42,48]. Lyon and Gan [42] studied thermo-responsive nanogels with a small range of tunable VPTT. Bae et al. [48] prepared non-ionic nanogels through copolymerization of a hydrophobic NIPA and more hydrophobic *N*-tert-butylacrylamide (NTBA). One may wonder how the incorporation of a large amount of hydrophilic co-monomer will affect the phase transition behavior of non-ionic co-polymer nanogels. As shown in Fig. 4a, the phase transition behavior of the DEA/DMA nanogels varies tremendously with different hydrophilic DMA content. Specifically, while homogeneous polyDEA nanogels undergo a sharp volume-phase transition with a VPTT at 26 °C, an increase in the DMA content results in an increase of the VPTT of the DEA–DMA co-polymer nanogels. The corresponding decrease in the size of the DEA/DMA nanogels above the VPTT (Fig. 4a) shows that DEA/DMA nanogels over this wide range of compositions are stable and undergo no aggregation in dilute aqueous solution above the VPTT over this wide range of compositions.

Fig. 4a also shows that in contrast to the behavior of the polyDEA nanogels, the DEA/DMA nanogels exhibit broad phase transitions and a lower extent of volume collapse with temperature. The differing phase transition behavior of the DEA/DMA nanogels is most likely due to the different hydrophilic/hydrophobic balance of the random copolymer chains. Baker and coworkers [39] studied the conformational transitions of linear NIPA/DMA copolymers in aqueous solution using time-resolved anisotropy measurements (TRAMS), fluorescence quenching, and pyrene solubilization. They found that increasing the DMA content resulted in the adoption of increasingly open conformations above the respective LCSTs of linear NIPA/DMA copolymers. Thus, NIPA/DMA copolymers exhibit broad collapse transitions and more flexible globules above the LCST, with an increase of the DMA content. The DEA/DMA copolymer chains in the nanogels would be expected to show similar phase transition behaviors.

To summarize, our results demonstrate that increasing the DMA content of the DEA/DMA nanogels leads to a higher VPTT, lower swelling ratio, and increasingly broad phase transitions. This can be clearly seen in Fig. 4b, which shows the normalized change in hydrodynamic diameter, D_h/D_{ho}, as a function of temperature, where D_h is an average diameter of nanogels as a function of temperature and D_{ho} is an average diameter of nanogels at 20 °C.

In the discussion above, DLS studies revealed the phase transition behaviors of very dilute nanogel dispersions. For semi-dilute and concentrated nanogel dispersions, visible-light absorption spectrophotometry is a powerful tool to optically study phase transitions and aggregation. As nanogel dispersions undergo a

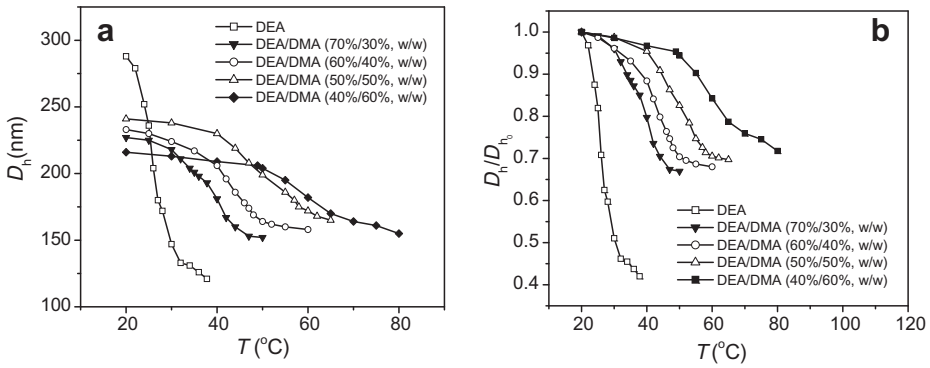

Fig. 4. (a) The volume-phase transition of polyDEA and DEA/DMA nanogels with four different compositions (70%/30%, 60%/40%, 50%/50%, and 40%/60%, w/w). D_h is an average diameter of nanogels as a function of measured temperature and D_{ho} is an average diameter of nanogels at 20 °C. (b) The de-swelling ratio of polyDEA and DEA/DMA nanogels with four different compositions (70%/30%, 60%/40%, 50%/50%, and 40%/60%, w/w).

thermo-responsive phase transition, the nanogels collapse and the turbidity of the dispersions significantly increases. We utilized visible-light absorption spectrophotometry to study the effects of varying heating rates, nanogel concentrations, and salt concentrations on the phase transition behaviors of DEA/DMA nanogels. In principle, the thermodynamic equilibrium VPTT of the DEA/DMA nanogels is dependent only on the composition and concentration of the nanogels and the solvent. But studies of the heating rate dependence of the phase transition can provide insight into the dynamic transition process of nanogel dispersions and allow users to choose optimal heating rates for applications or other further investigations [20,49]. For a 1 wt.% DEA/DMA (70%/30%, w/w) nanogel aqueous solution, heating rates were varied from 5 to 0.2 °C/min. As illustrated in Fig. 5a, increasing the heating rate over this range results in a shift of the dynamic VPTT from 47 to 53 °C, with an essentially linear dependence on heating rate (Fig. 5b). At high heating rates, nanogels exhibit a higher dynamic VPTT, possibly due to the delayed equilibrium time for transferring heat through the dispersion and nanogel networks.

Fig. 5b shows that the difference in the VPTT between 0.2 °C/min and 2 °C/min is only about 1.5 °C. In order to facilitate measurement, we choose the heating rate of 2 °C/min for subsequent visible-light spectrophotometry studies of the phase transitions. In more concentrated dispersions, nanogel–nanogel hydrophobic interactions must be considered in studying the phase transition behavior. Fig. 6 shows the dramatic effect of concentration on the phase transition behavior of DEA–DMA (70%/30%) nanogels. The results show that an increase in concentration from 1 to 4 wt.% results in a lower apparent VPTT and a sharper phase transition. At higher concentrations of 4 wt.% and 8 wt.%, the nanogel solutions exhibited no difference in their phase transition behavior. The very sharp phase transitions seen for higher concentrations may be due to a very rapid and strong aggregation of the nanogels. The results discussed above show that the heating rate and concentration strongly influence both the dynamic VPTT and the phase transition kinetics of DEA/DMA nanogels.

3.4. Salt Effects

The effects of salt on water-soluble polymers or hydrogels are of great importance and of great interest because salts are present in numerous biological systems. As early as 1888, Hofmeister reported the "salting-out" effect of egg-white protein [50]. "Salting-out" effects may be explained by the salt-induced disruption of the tetrahedral structure of water [51,52]. Salt-induced phase transitions of non-ionic polymer gels [53] and microgels [54,55] have been studied by others. The salts used were inorganic salts such as NaCl, KCl, and additionally $CaCl_2$ and organic salts such as H_4NBr, $(n\text{-}C_5H_{11})_4NBr$, and the surfactants SDS and DTAB (dodecyltrimethylammonium bromide) were studied. The addition of inorganic salts generally results in a shift of the VPTT of the polymer gels to lower temperature [53]. The effect of added organic salts on the VPTT depends on the alkyl chain length [56], where some of the salts raise the VPTT and the others lower the VPTT.

Salt effects on thermosensitive, non-ionic gels studied by others mainly focus on homogeneous polymer gels such as NIPA gels [54]

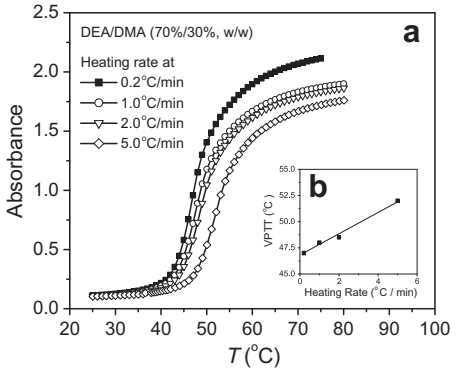

Fig. 5. (a) The turbidity changes of DEA/DMA nanogels (70%30%, w/w) with temperature at different heating rates (0.2 °C/min, 1 °C/min, 2 °C/min, and 5 °C/min). (b) Effect of heating rate on the dynamic VPTT of the DEA/DMA (70%/30%, w/w) nanogels.

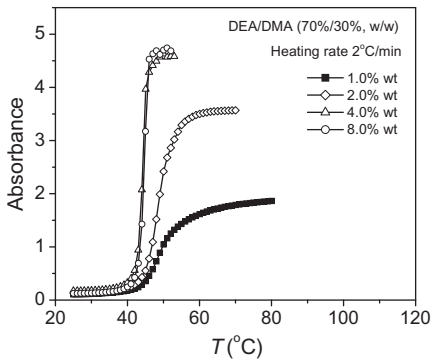

Fig. 6. The phase transition behavior of DEA/DMA nanogels (70%/30%, w/w) with temperature at nanogel concentrations of 1.0 wt.%, 2.0 wt.%, 4.0 wt.%, and 8.0 wt.% at heating rate of 2 °C/min.

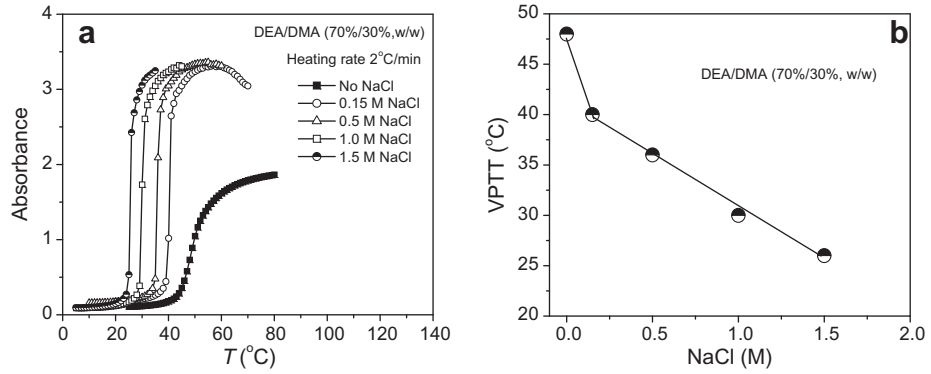

Fig. 7. (a) The turbidity changes of the DEA/DMA (70%/30%, w/w) nanogels with temperature at different NaCl concentrations of 0.15 M, 0.5 M, 1.0 M, and 1.5 M. Turbidities were measured at heating rate of 2 °C/min. (b) Effect of NaCl concentration on the VPTT of the DEA/DMA (70%/30%, w/w) nanogels. Turbidities were measured at heating rate of 2 °C/min.

and hydroxypropylcellulose gels [3]. We investigated the NaCl-induced phase transition behavior of non-ionic DEA/DMA co-polymer nanogel dispersions that had different compositions of hydrophilic DMA and hydrophobic DEA. The effect of salt concentration on the phase transition behavior of 1 wt.% DEA-DMA (70%/30%) nanogels was also studied. Fig. 7a shows that the VPTT of the DEA/DMA nanogels decreases with an increase of NaCl concentration, while the extent of aggregation for the nanogels is much greater than that observed in pure water.

In contrast to the stable nanogel dispersions we observe in aqueous solutions without NaCl, even at just 0.15 M NaCl, the DEA/DMA nanogels quickly formed a macroscopic precipitate above the VPTT. Fig. 7b shows the strong effects of NaCl concentration on VPTT. This result shows that NaCl not only decreases the VPTT, but also greatly increases the tendency of nanogels to aggregate, presumably by screening ionic repulsions that stabilize the nanogels in aqueous solution. The salt-induced volume-phase transition and aggregation at temperatures above the VPTT may also be related to NaCl-induced disruption of water structure [51,52,56]. In order to monitor the salt effect on the size change and stability of individual nanogels, one requires a very dilute nanogel solution. Vincent et al. studied the salt-induced aggregation of polyNIPA microgels using DLS [55]. They found that at low salt concentrations (<0.2 M), polyNIPA microgels coagulate at a higher temperature. Moreover, they found that polyNIPA microgels coagulated in 1 M NaCl at 42 °C but did not phase-separate to form sediment. In this work, stronger coagulation was similarly observed at a low salt concentration, as shown in Fig. 8. At the physiological salt concentration of 0.9 wt.% (154 mM), DEA/DMA (70%/30%, w/w) nanogels coagulate at 39 °C. However, the coagulated nanogels did not aggregate to form a macroscopic precipitate. Upon subsequent cooling below the phase transition temperature, the coagulated nanogels re-dispersed in salt solution to form a stable solution.

Aqueous dispersions of polyDEA and DEA/DMA nanogels exhibit different optical appearances, as shown in Fig. 9. Similar to polyNIPA nanogel dispersions [57], polyDEA nanogel dispersions are opaque at 1 wt.% (Fig. 9a) and deep blue at 6 wt.% (Fig. 9b). In contrast to polyDEA nanogel dispersions, DEA/DMA nanogel dispersions exhibit a light blue color at 1 wt.% (Fig. 9c). At a low concentration of 1 wt.%, DEA/DMA nanogels dispersed in water and an interface exists between nanogels. Due to loosely packed polymer chains in individual nanogels, the refractive index of an individual nanogel is a little bit higher than that of water. Such a small refractive index difference between water and nanogels leads to a light blue dispersion in color. However, at the high concentration of 8 wt.% (Fig. 9d), the interface between DEA/DMA nanogels disappears due to the interchain entanglement of the loosely packed polymer chains between the nanogels. Therefore, just like water-soluble polymer solution, DEA/DMA nanogel dispersions demonstrate an optical transparency, which only occur at a very high concentration (14 wt.%) of polyNIPA dispersions [57]. Such optically clear, concentrated DEA/DMA nanogel dispersions in aqueous media could find useful applications, for example as DNA separation media for

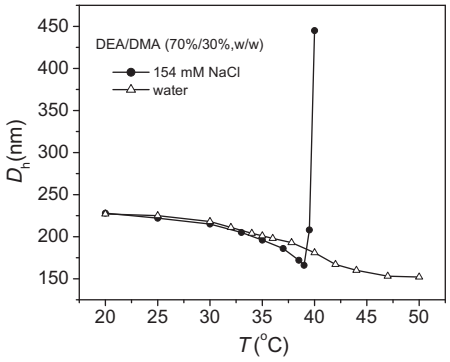

Fig. 8. The phase transition behavior of an ultra-dilute DEA/DMA (70%/30%, w/w) nanogel solution (1.2×10^{-5} g/ml) with temperature in water and in the physiological salt concentration of 154 mM NaCl.

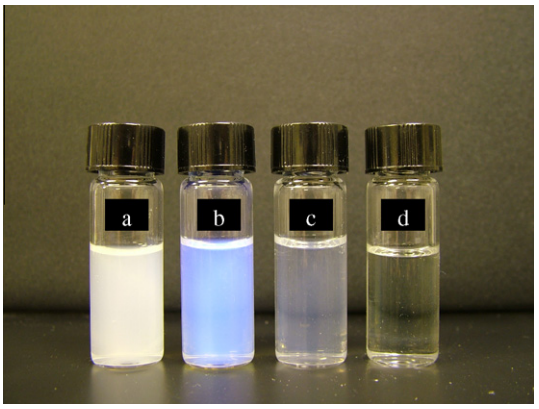

Fig. 9. The optical appearances of polyDEA and DEA/DMA (40%/60%, w/w) nanogel aqueous dispersions at different concentrations at 20 °C from left to right (a) polyDEA nanogels (1 wt.%), (b) polyDEA nanogels (6 wt.%), (c) DEA/DMA nanogels (1 wt.%), (d) DEA/DMA nanogels (8 wt.%).

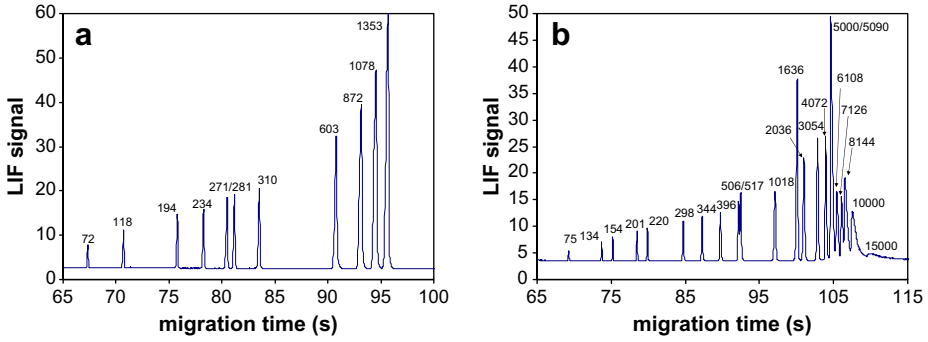

Fig. 10. Separation of dsDNA by microfluidic electrophoresis of *Φ*X174 RF DNA/*Hae* III Fragments (A) and 1 Kb DNA Extension Ladder (B). (a) In a blended polymer matrix of two molar mass of HEC (27 kDa, 0.84%; 1 MDa, 0.21%) and one high-molar mass of LPA (7 MDa, 0.09 wt.%) with addition of DEA/DMA (40%/60%. wt.%/wt.%) nanogel (xl1451, 0.6 wt.%) the resolution between fragments of 271/281 was 2.22 which is greatly improved from 1.03 without the addition of DEA/DMA nanogel. The peaks from left to right are assigned to 72, 118, 194, 234, 271/281, 310, 603, 872, 1078, 1353 bp in *Φ*X174 RF DNA/*Hae* III Fragments, (b) In a pure DEA/DMA nanogel (xl1453, 2.7 wt.%) solution, fragments in 1 Kb DNA Extension Ladder are separated up to 15,000 bp. The peaks from left to right are assigned to 75, 134, 154, 201, 220, 298, 344, 396, 506/517, 1018, 1636, 2036, 3054, 4072, 5000/5090, 6108, 7126, 8144, 10,000, 15,000.

capillary and chip-based electrophoresis, which requires transparent polymer solutions.

DEA/DMA nanogel solutions were also tested as a novel component in sieving matrices for dsDNA separations by microfluidic electrophoresis. In 1993–1996, Barron et al. [58] showed that ultra-dilute solutions of hydroxyethylcellulose (HEC) could serve as useful separation media for capillary electrophoresis of relatively large double-stranded (ds) DNA molecules (>1000 bp in size). Many other polymer systems have been investigated for DNA separations with good resolution over a wide range of size (i.e., from tens of DNA bp up to tens of thousands of DNA bp). A blended polymer matrix of HEC that comprised an optimized mixture of low- and high-molar mass HEC polymers showed superior peak separations over a wide range of DNA fragments, from 72 bp to 23.1 kbp [59]. It was found that more concentrated low molar mass HEC was appropriate for separating small DNA fragments, while dilute high-molar mass HEC is appropriate for larger DNA fragments. Our group has identified an optimal blended polymer matrix for DNA sizing for fragments ranging from 75 bp up to 12 kbp; the mixture consisted of HEC of two different average molar masses (27 kDa, 0.84%; 1 MDa, 0.21%) with high-molar mass LPA (7 MDa, 0.09 wt.%) through an orthogonal design of experiment. With the addition of DEA/DMA co-polymer nanogels (40% DEA/60% DMA, w/w) to this blended polymer matrix, a much further improved DNA separation performance could be achieved by microfluidic chip electrophoresis for *Φ*X174/*Hae* III restriction fragments. The resolution between fragments 271/281 was calculated using an exponentially modified Gaussian (EMG) model and PeakFit ver. 4.0. The peak resolution increased from 1.03 without DEA/DMA co-polymer nanogels to 1.82, 1.97, and 2.22 upon the addition of DEA/DMA co-polymer nanogels at concentrations of 0.1 wt.%, 0.3 wt.% and 0.6 wt.% respectively. Fig. 10a shows the electropherogram for *Φ*X174/*Hae* III DNA restriction fragments in the blended polymer matrix with 0.6 wt.% DEA/DMA co-polymer nanogels. We are able to discern distinct peaks for the 271/281 dsDNA fragment pair, which normally is quite challenging to obtain. Fig. 10b shows the separation of a 1 kbp dsDNA "ladder"-type sample in a pure DEA/DMA nanogel solution at 2.7% w/w. An ultrafast, high-efficiency separation is achieved in less than 120 s, covering a broad range of DNA sizes (75 bp up to 15,000 bp). Therefore, novel DEA/DMA co-polymer nanogels promise to be a useful component of complex blended polymer matrices that enable enhanced separations of large DNA fragments without losing an ability to resolve small DNA molecules. Previous reports including static "obstacles" in microfabricated entropic trap (ET) array [60] and dynamic "obstacles" of packed nanospheres with applied pressure [8] facilitated the separation of relatively large dsDNA molecules, which separations that similar to those that we present here. Although the true mechanism of this separation enhancement is not yet understood, it demonstrates a practical application for DEA/DMA co-polymer nanogels as a key component of sieving media for dsDNA separations. The nanogel solutions offer some advantages over ET arrays, which cannot be changed or tuned after their fabrication; nanogel-enhanced sieving media can be tuned to provide particular DNA separations by changing the solution composition.

4. Conclusions

Non-ionic polyDEA nanogels and DEA/DMA nanogels with four different DEA/DMA co-monomer compositions (70%/30%, 60%/40%, 50%/50%, and 40%/60%, w/w) were synthesized by emulsion precipitation polymerization with and without added surfactant, respectively. This is the first report of thermo-responsive, non-ionic co-polymer nanogels with high hydrophilic co-monomer compositions made by emulsion precipitation polymerization. DEA/DMA nanogels can only be synthesized at a temperature just a few degrees above the initial phase transition temperature, and the ideal reaction temperature is typically a few degrees above the respective initial phase transition temperature. In a range of reaction temperatures, higher synthesis temperature results in the formation of larger nanogels. The average size of the nanogels also increases with an increase in the crosslinker concentration, whereas the size distribution of the nanogels varied little for the different synthesis conditions studied.

The weight-average molecular weights (M_w) of the resultant DEA/DMA nanogels were measured by static MALLS. In contrast to the highly packed polymer chains in polyDEA nanogels, DEA/DMA nanogels with four different compositions consist of more loosely packed polymer chains. The phase transition behaviors of DEA/DMA nanogels were studied using both dynamic light scattering and visible-light spectrophotometry. Compared to homogeneous polyDEA nanogels, DEA/DMA nanogels exhibit relatively broad volume-phase transitions around their individual VPTTs, and a lower extents of collapse. The VPTT and swelling ratio of DEA/DMA nanogels are dependent on the composition of the nanogels. A higher hydrophilic DMA content results in a higher VPTT and a lower swelling ratio. The variation of the VPTT and swelling ratio is due to different hydrophilic/hydrophobic balance. In addition to the composition of DEA/DMA nanogels, the variation of heating rate, nanogel concentration, and salt concentration can

strongly affect the phase transition behavior. The dynamic VPTTs of DEA/DMA nanogels increases with an increase of heating rate. A higher nanogel concentration (4 wt.% and 8 wt.%) leads to a much sharper phase transition and lower dynamic VPTT, as compared to results at a lower concentration (1 wt.% and 2 wt.%). It was expected that NaCl would induce a decrease in the VPTT of DEA/DMA nanogels, and this was indeed observed. Moreover, NaCl leads to a much sharper phase transition of DEA/DMA nanogels in a semi-dilute solution. DEA/DMA nanogels are stable in dilute aqueous dispersion above the VPTT, but are unstable and coagulate to form large particles even in an ultra-dilute nanogel solution (1.2×10^{-5} g/ml) at a physiological 154 mM NaCl concentration. However, the coagulation of the nanogels in this solution condition is reversible, and they can be dissociated into stable nanogel dispersions below the VPTT.

In contrast to the opaque or colored dispersions of polyDEA nanogels, DEA/DMA nanogels exhibit optically clear dispersions in aqueous media when dissolved at high concentrations. When DEA/DMA nanogel dispersions were used in separation matrices for microchip electrophoresis in borosilicate glass microfluidic devices, they provided fast, beautiful separations of dsDNA ranging from 72 bp to 15,000 bp in size.

Acknowledgments

We thank Dr. Christopher Fredlake and Dr. Daniel Hert for helpful comments. We acknowledge Dr. Cheuk-Wai Kan and Dr. Erin A. Doherty's technical assistance and support by the National Institutes of Health (1 R01 HG 019770). XL acknowledges support from Northwestern's NSF/NSEC program of NSF-EEC-0118026 and the DURINT program of Air Force Office of Scientific Research (F49620-01-0401). CWK and AEB acknowledge support from the MRSEC program of the National Science Foundation (DMR-0076097) at the Materials Research Center, Northwestern University.

Appendix A. Supplementary material

Supplementary data associated with this article can be found, in the online version, at doi:10.1016/j.jcis.2011.01.079.

References

[1] C. Scherzinger, P. Lindner, M. Keerl, W. Richtering, Macromolecules 43 (2010) 6829.
[2] X. Hu, Z. Tong, L.A. Lyon, J. Am. Chem. Soc. 132 (2010) 11470.
[3] X. Lu, Z. Hu, J. Gao, Macromolecules 33 (2000) 8698.
[4] R.H. Pelton, Adv. Colloid Interface Sci. 85 (2000) 1.
[5] S. Zhou, B. Chu, J. Phys. Chem. B 102 (1998) 1364.
[6] K. McAllister, P. Sazani, M. Adam, M.J. Cho, M. Rubinstein, R.J. Samulski, J.M. DeSimone, J. Am. Chem. Soc. 124 (2002) 15198.
[7] S.V. Vinogradov, E.V. Batrakova, A.V. Kabanov, Bioconjugate Chem. 15 (2004) 50.
[8] M. Tabuchi, M. Ueda, N. Kaji, Y. Yamasaki, Y. Nagasaki, K. Yoshikawa, K. Kataoka, Y. Baba, Nat. Biotechnol. 22 (2004) 337.
[9] G.E. Morris, B. Vincent, M.J. Snowden, J. Colloid Interface Sci. 190 (1997) 198.
[10] M.J. Serpe, J. Kim, L.A. Lyon, Adv. Mater. 16 (2004) 184.
[11] C.E. Reese, A.V. Mikhonin, M. Kamenjicki, A. Tikhonov, S.A. Asher, J. Am. Chem. Soc. 126 (2004) 1493.
[12] K. Ogawa, A. Nakayama, E. Kokufuta, Langmuir 19 (2003) 3178.
[13] J.S. Lowe, B.Z. Chowshry, J.R. Parsonage, M.J. Snowden, Polymer 39 (1998) 1207.
[14] D. Duracher, A. Elaissari, C. Pichot, Polym. Sci., Part A Polym. Chem. 37 (1999) 1823.
[15] D. Gan, L.A. Lyon, J. Am. Chem. Soc. 123 (2001) 8203.
[16] S. Kazakov, M. Kaholek, I. Teraoka, K. Levon, Macromolecules 35 (2002) 1911.
[17] K. Ogawa, A. Nakayama, E. Kokufuta, J. Phys. Chem. B 107 (2003) 8223.
[18] S. Ito, K. Ogawa, H. Suzuki, B. Wang, R. Yoshida, E. Kokufuta, Langmuir 15 (1999) 4289.
[19] L. Taylor, L. Cerankowski, J. Polym. Sci., Polym. Chem. Ed. 13 (1975) 2551.
[20] I. Idziak, D. Avoce, D. Lessard, D. Gravel, X. Zhu, Macromolecules 32 (1999) 1260.
[21] M. Siu, H. Liu, X.X. Zhu, C. Wu, Macromolecules 36 (2003) 2103.
[22] M. Colonne, Y. Chen, S. Wu, S. Freiberg, S. Giasson, X.X. Zhu, Bioconjugate Chem. 18 (2007) 999.
[23] B.A. Buchholz, E.A. Doherty, M.N. Albarghouthi, F.M. Bogdan, J.M. Zahn, A.E. Barron, Anal. Chem. 73 (2001) 157.
[24] H. He, B.A. Buchholz, L. Kotler, A.W. Miller, A.E. Barron, B.L. Karger, Electrophoresis 23 (2002) 1421.
[25] W. Wu, J. Shen, P. Banerjee, S. Zhou, Biomaterials 31 (2010) 7555.
[26] T. Zhou, W. Wu, S. Zhou, Polymer 51 (2010) 3926.
[27] F.D. Jochum, L. Zur Borg, P.J. Roth, P. Theato, Macromolecules 42 (2009) 7854.
[28] F.D. Jochum, P.J. Roth, D. Kessler, P. Theato, Biomacromolecules 11 (2010) 2432.
[29] J. Zhang, H. Chen, L. Xu, Y. Gu, J. Controlled Release 131 (2008) 34.
[30] R.H. Pelton, P. Chibante, Colloids Surf. 20 (1986) 247.
[31] M. Chiari, C. Micheletti, M. Nesi, M. Fazio, P.G. Righetti, Electrophoresis 15 (1994) 177.
[32] V. Barbier, J.L. Viovy, Curr. Opin. Biotechnol. 14 (2003) 51.
[33] E.A. Doherty, K.D. Berglund, B.A. Buchholz, I.V. Kourkine, T.M. Przybycien, R.D. Tilton, A.E. Barron, Electrophoresis 23 (2002) 2766.
[34] B. Chu, Laser Light Scattering, 2nd ed., Academic Press, New York, 1991.
[35] W. Brown, Dynamic Light Scattering, Oxford Science Publications, 1993.
[36] T.N. Chiesl, W. Shi, A.E. Barron, Anal. Chem. 77 (2005) 772–779.
[37] R.H. Pelton, P. Chibante, Colloids Surf. 20 (1986) 247.
[38] K. Tam, X. Wu, R.H. Pelton, Polym. Sci., Part A Polym. Chem 31 (1993) 963.
[39] I.C. Barker, J.M. Cowie, T.N. Huckerby, D.A. Shaw, I. Soutar, L. Swanson, Macromolecules 36 (2003) 7765.
[40] C. Wu, Polymer 39 (1998) 4609.
[41] C. Wu, X.H. Wang, Phys. Rev. Lett. 80 (1998) 4092.
[42] D. Gan, L.A. Lyon, Macromolecules 35 (2002) 9634.
[43] J. Gao, B. Frisken, Langmuir 19 (2003) 5217.
[44] D. Duracher, A. Elaissari, C. Pichot, Macromol. Symp. 150 (2000) 305.
[45] G. Chen, A.S. Hoffman, Nature 373 (1995) 49.
[46] Y.C. Bae, D. Soane, J. Chromatogr. 652 (1993) 17.
[47] M.N. Albarghouthi, A.E. Barron, Electrophoresis 21 (2000) 4096.
[48] Y.D. Yi, Y.C. Bae, J. Appl. Polym. Sci. 67 (1998) 2087.
[49] L. Li, H. Shan, C.Y. Yue, Y.C. Lam, K.C. Tam, X. Hu, Langmuir 18 (2002) 7291.
[50] F. Hofmeister, Arch. Exp. Path. Pharmakol. 24 (1888) 247.
[51] R. Leberman, A.K. Soper, Nature 378 (1995) 364.
[52] B. Hribar, N.T. Southall, V. Vlachy, K.A. Dill, J. Am. Chem. Soc. 124 (2002) 12302.
[53] T. Park, A.S. Hoffman, Macromolecules 26 (1993) 5045.
[54] E. Daly, B.R. Saunders, Langmuir 16 (2000) 5546.
[55] A.F. Routh, B. Vincent, Langmuir 18 (2002) 5366.
[56] H. Inomata, S. Goto, K. Otake, S. Saito, Langmuir 8 (1992) 687.
[57] J. Gao, Z. Hu, Langmuir 18 (2002) 1360.
[58] A.E. Barron, D.S. Soane, H.W. Blanch, J. Chromatogr. A 652 (1993) 3.
[59] A.P. Bunz, A.E. Barron, J.M. Prausnitz, H.W. Blanch, Ind. Eng. Chem. Res. 35 (1996) 2900.
[60] J. Han, H.G. Craighead, Science 288 (2000) 1026.